

# THREE PHASE INDUCTION MOTOR INCIPIENT ROTOR'S FAULTS DETECTION BASED ON IMPROVED ROOT-MUSIC APPROACH

A .H.Boudinar, A.Bendiabdellah, N.Benouzza, N.Boughanmi

L.D.E.E Laboratory, Department of Electrical Engineering, Faculty of Electrical Engineering

University of Sciences and Technology of Oran, Algeria

E-mail: [boud\\_ah@yahoo.fr](mailto:boud_ah@yahoo.fr)

**Abstract** – Induction motor plays a very important role in industrial applications. Early fault detection is one of the main problems. So, in order to detect an incipient fault, we must pay a special attention to the spectral analysis of stator current. Several frequency estimation techniques have been developed and used to help induction motor fault detection and diagnosis. In this paper, a new application of the Root-MUSIC method to improve the diagnosis is proposed. This method is a variant of the well known MUSIC (Multiple Signal Classification) method. This is a powerful tool for extracting meaningful frequencies from the signal, which is in our case the stator current. Unfortunately, the Root-MUSIC method takes a long computation time to find more frequencies by increasing the order of the frequency signal dimension. To solve this problem, this method will not be applied to the totality of the signal spectrum but only to a bandwidth of specified frequency. An algorithm RMIF (Root-MUSIC Improved by Filtering) based on a digital pass-band filter within a specific frequency range is proposed with Root-MUSIC in order to improve the diagnosis performances. The proposed technique has been applied to detect incipient broken bar rotor faults in a three-phase squirrel-cage induction motor. Experimental results were presented to show the various merits of this RMIF technique compared to the classical PSD technique.

**Key words:** Broken bars, fault detection, induction motors, stator current, spectral estimation techniques, PSD, Root-MUSIC, pass-band filter

## 1. Introduction

Induction motors especially squirrel cage have a very important role in industry. They are robust and simple in their construction. However, an interruption of a manufacturing process due to a failure in an induction motor can induce a serious financial set for the company. It is therefore necessary to detect a faulty condition and avoid its increase, before resulting in a catastrophic failure. For this reason, the early detection of the incipient motor fault is very important [1]. Among the various faults, rotor faults account for about 10% of total

induction motor failures. Broken rotor bars can be a serious problem when induction motors (IM) have to perform hard duty cycles. Broken rotor bars do not initially cause an IM to fail, but they can cause serious mechanical damage to the stator windings if they are left undetected [2]. Moreover an IM with broken rotor bars cannot operate in dangerous environments due to sparking at the fault site. The techniques more efficient in identifying rotor faults are mainly based on analysis of stator currents via Fast Fourier Transform (FFT) algorithm. FFT yields efficient and reasonable results, which makes it a powerful tool as a diagnostic technique. Among these techniques, we have Power Spectral Density (PSD). There are several approaches to calculate PSD estimates. Periodogram technique, which is known as the classical way to estimate PSD, is one of these methods [3]. However, a main disadvantage of these techniques is the problem of resolution. Indeed, when we have two harmonics close one to the other with very different amplitudes, the lobe of the low amplitudes' harmonics will be buried in that of the main harmonic. In recent years, several advanced signal processing methods such as High Resolution Spectral Analysis have been applied to diagnose IM faults. Among these methods, Root-MUSIC algorithm has been used both to distinguish the fundamental frequency and the twice slip frequency side bands caused by broken rotor bars. In this application, fault sensitive frequencies have to be found in the stator current signature. They are often numerous in a given frequency range and they are affected by the signal-to-noise ratio. In this condition, the Root-MUSIC method takes a long computation time to find more frequencies by increasing the order of the frequency signal dimension. To solve this problem, the idea is to focus on some special frequency bins without taking care of the full length FFT in the entire frequency range. Using this idea, one can obtain [4] not only a computation time reduction and more memory space

saving, but also a good accuracy in a specified frequency range. In this paper, an algorithm is being proposed; based on the *Root-MUSIC* combined to a digital pass-band filtering applied within a specified frequency range; in order to improve diagnosis performances. The experimental results obtained with this algorithm *RMIF* will be compared with the classical spectral estimation *PSD* technique.

## 2. Stator Current Signature Analysis

A current spectrum contains potential fault information. Frequency components have been determined for each specified fault. These frequencies are derived from the physical construction of the machine. It is important to note that, as in vibration analysis case, the more the fault progresses, its characteristic spectral components continue to increase with time [5]. *Kliman*, *Elkasabgy* [6], [7] used motor current signature analysis techniques to detect broken rotor bar faults by investigating the sideband components around the supplied current fundamental frequency (i.e. line frequency),  $f_s$ . Broken rotor bars give rise to a sequence of side-bands given by [1], [3]:

$$f_b = (1 \pm 2.k.s).f_s \quad \text{with } k=1,2,3... \quad (1)$$

Where  $f_b$  are the sideband frequencies associated with the broken rotor bar,  $s$  is the per unit motor slip [3], given by:

$$s = \frac{w_s - w_r}{w_s} \quad (2)$$

$w_r$  is the relative mechanical speed of the motor. The motor synchronous speed,  $w_s$ , is related to the line frequency  $f_s$ , as:

$$w_s = \frac{120.f_s}{P} \quad (3)$$

Where  $P$  is the number of poles of the motor.

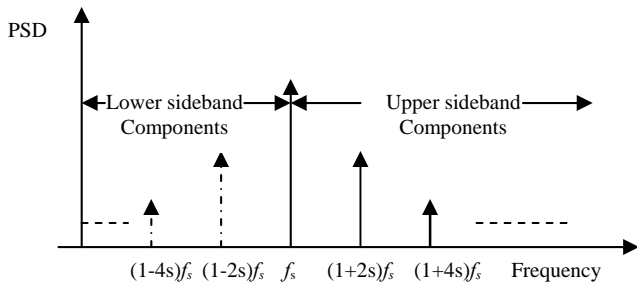


Fig.1. Sideband frequencies around the fundamental line frequency

Figure1 shows the frequency components specific to broken rotor bar fault, as given in equation (1) for  $k=1$  and 2. These frequencies are located around the

fundamental line frequency and are called lower sideband and upper sideband components.

In addition with the previous equation, broken rotor bars generate additional sidebands near the space harmonics frequencies [8], given by:

$$f_{rsb} = f_s \left[ \frac{k}{P} (1-s) \pm s \right], \quad \text{with } k/P=1, 3, 5... \quad (4)$$

The evolution of these sidebands magnitudes makes an efficient diagnosis of induction motor possible.

## 3. Root-MUSIC Method

### 3.1. Basic Theory

*Root-MUSIC* method is generally used in signal processing problems. This method estimates the frequencies of the complex sinusoids that best approximate a noisy signal by using an eigen based decomposition method [9], [10], [11]. Let us consider a stator current  $i_s(n)$  as a sum of  $L$  complex sinusoids and white noise:

$$i_s(n) = \sum_{i=1}^L I_i e^{j(2\pi \cdot \frac{f_i}{f_{sf}} \cdot n + \phi_i)} + w(n) \quad (5)$$

With  $n=0, 1, 2, \dots, N-1$ . And where  $I_i$ ,  $f_i$ , and  $\phi_i$  are the amplitude, the frequency and the random phase of the  $i^{\text{th}}$  complex sinusoid (harmonic components) respectively,  $w(n)$  is white noise,  $f_{sf}$  sampling frequency and  $N$  is the number of sample data.

The autocorrelation matrix of the noisy signal  $i_s$  is the sum of the autocorrelation matrices of the signal  $i_s$  and the noise  $w$  defined as follows:

$$R_i = E[i_s(n).i_s^H(n)] = R_s + R_w = S.A.S^H + \sigma_w^2.I \quad (6)$$

Where:

-  $S$  is the Vandermonde matrix:

$$S = [s_1 \dots s_i \dots s_L] \quad (7)$$

$$s_i = [1 \ e^{j.2\pi \cdot \frac{f_i}{f_{sf}}} \ e^{j.4\pi \cdot \frac{f_i}{f_{sf}}} \ \dots \ e^{j.2\pi(N-1) \cdot \frac{f_i}{f_{sf}}}]^T$$

-  $A$  is the power matrix of the harmonics.

$$A = \text{diag}[I_1^2 \ I_2^2 \ \dots \ I_L^2] \quad (8)$$

-  $H$  is the Hermitian transpose.

-  $\sigma_w^2$  and  $I$  are respectively the variance of the white noise and the identity matrix of size  $(N \times N)$ .

The eigen decomposition of the autocorrelation matrix  $R_i$  is given by:

$$R_i = \sum_{k=1}^N \lambda_k u_k u_k^H = \underbrace{U_s \cdot D_s \cdot U_s^H}_{R_s} + \underbrace{U_w \cdot D_w \cdot U_w^H}_{R_w} \quad (9)$$

$$\begin{aligned} U_s &= [u_1 \ \dots \ u_L] ; D_s = \text{diag}[\lambda_1 \ \dots \ \lambda_L] \\ \text{Where: } U_w &= [u_{L+1} \ \dots \ u_N] ; D_w = \sigma_w^2 I_{N-L} \end{aligned} \quad (10)$$

$U_s$  and  $U_w$  matrices are composed by the eigen vectors  $u_k$  related to eigen values arranged in descending order. This equation shows that, we may divide these eigenvectors into two groups or subspaces: the  $L$  signal eigen vectors corresponding to the  $L$  largest eigen values (signal subspace), and  $N-L$  noise eigen vectors that, ideally, have eigen values equal to  $\sigma_w^2$  (noise subspace). Diagonal matrices  $D_s$  and  $D_w$  contain eigen values  $\lambda_k$  corresponding to eigen vectors  $u_k$ .

As the eigen values of noise are equal to the variance of noise, matrix  $D_w$  can be written as shown in equation (10). By comparing equations (6), (9) and (10) we can write:

$$\begin{aligned} R_i.U_w &= U_w.D_w = \sigma_w^2.D_w \\ &= S.A.S^H.U_w + \sigma_w^2.U_w \end{aligned} \quad (11)$$

$$\text{This implies that: } S^H.U_w = 0 \quad (12)$$

The *Root-MUSIC* method uses the principle of this orthogonality between the signal subspace and the noise subspace. The required frequency

estimates  $z_i = e^{j.2\pi.\frac{f_i}{f_{sf}}}$  are the roots of this equation [11]:

$$s_i^H U_w U_w^H s_i = 0 \quad \text{with } i=1, \dots, L \quad (13)$$

The roots of (13) will come in pairs (i.e. if  $z_i$  is a root, so is  $(1/z_i^*)$ ). Those roots with magnitude greater than unity will be filtered out. The  $L$  roots closest to the unit circle correspond to possible harmonics according to:

$$f_i = \frac{f_{sf}}{2\pi} \cdot \arg(z_i) \quad \text{with } i=1, \dots, L \quad (14)$$

### 3.2. Harmonics Powers Estimation

Knowing that:

$$R_s = S.A.S^H = \sum_{k=1}^L (\lambda_k + \sigma_w^2) u_k u_k^H \quad (15)$$

We notice that it is easier to inverse  $R_s$  than to inverse  $S$ . Therefore the harmonics powers can be estimated by the following method [11], [12]:

$$Q = A^{-1} = \frac{1}{S^H R_s^{-1} S} \quad (16)$$

$$\text{Where: } \begin{cases} R_s^{-1} = \sum_{k=1}^L \frac{1}{\lambda_k + \sigma_w^2} u_k u_k^H \\ \sigma_w^2 = \frac{1}{N-L} \sum_{k=L+1}^N \lambda_k \end{cases} \quad (17)$$

Identification problem is resolved by knowing the frequencies and the powers of the various harmonics.

Furthermore, the rank of the signal subspace determines the number of harmonics that is the eigenvectors spanning this subspace which allows us to estimate the frequency set. Due to the finite data length, we can not precisely compute the correlation matrix  $R_i$ . However, it is possible to estimate it [11]:

$$\hat{R}_i = \frac{1}{N-M+1} D.D^H \quad (18)$$

Where  $D$  is a Hankel data matrix given by:

$$D = \begin{bmatrix} i_s(0) & \dots & i_s(N-M) \\ \vdots & \ddots & \vdots \\ i_s(M-1) & \dots & i_s(N-1) \end{bmatrix}$$

$M$  is the data matrix order.

### 3.3. Choice of $L$ and $M$ Parameters

Obviously, this estimator requires the a priori knowledge of the number of frequencies  $L$  (model order) and the autocorrelation data matrix order  $M$ . For  $M$ , there is no rule to determine it. But some authors use empirically the parameter  $M$ , between  $N/2$  and  $N/3$  [13].

If the model order that is used is too small, then we will have less harmonics (an under estimation). If, on the other hand, the model order is too large, then the spectrum may contain spurious harmonics (an over estimation). Therefore, it would be useful to have a criterion that indicates the appropriate model order to use for a given set of data [14]. Among these criteria, we can quote the Akaike Information Criterion (*AIC*) [15] and the Minimum Description Length (*MDL*) proposed by Rissanen [16]. In this work, we have used the *AIC* criterion.

### 4. Improvement of Root-MUSIC Method

Actually, it is difficult to find out small magnitude frequencies around the main ones by the *Root-MUSIC* method because it takes a long computation time when the order of the autocorrelation matrix and the number of sample data increases. This computation time depends on  $N^3$  compared with  $N \log_2 N$  for the conventional FFT [10]. The suggested idea consists to process the data on a given frequency bandwidth and not on all the spectrum of the stator current, this will enables us to reduce the computation time and to optimize the

frequency component estimation. For example, in a three-phase induction machine with broken rotor bars, the side-band frequencies around the fundamental are important for fault detection [1], [4]. The proposed algorithm *RMIF* is based on a band-pass filter  $[f_l, f_h]$  where  $f_l, f_h$  are the low cut-off and high cut-off frequency of the band-pass filter respectively. Initially, the sequence  $i_s(n)$  is obtained after sampling the signal  $i_s(t)$  at the frequency  $f_{sf}$ . So, it would be possible to make a filtering in the bandwidth  $[0, f_{sf}/2]$ . However, the band-pass filter must have a flat response in the given bandwidth. After filtering, the frequency range becomes  $[f_l, f_h]$ . Therefore with this approach, the new sequence  $i_{sf}(n)$  has  $(2.N.f_p / f_{sf})$  samples, where  $f_p = f_h - f_l$ , reducing consequently the frequency signal dimension order for a reduced computation time in the frequency estimation for the given bandwidth. In addition, the rotor faults signature exists practically on each phase current spectrum. To make a diagnosis on each phase current will be penalizing in computation time. For this reason, we proposed the spectral analysis of the combination of the three phase currents, represented by the direct component  $i_{sd}$  [1], [17].

$$I_{sd} = \frac{I_a + \alpha I_b + \alpha^2 I_c}{3} \quad (19)$$

Where:  $\alpha = e^{j\frac{2\pi}{3}}$ ,  $I_a, I_b, I_c$  are the spectra of the three phases currents, and  $I_{sd}$  is a spectrum of direct component  $i_{sd}$ .

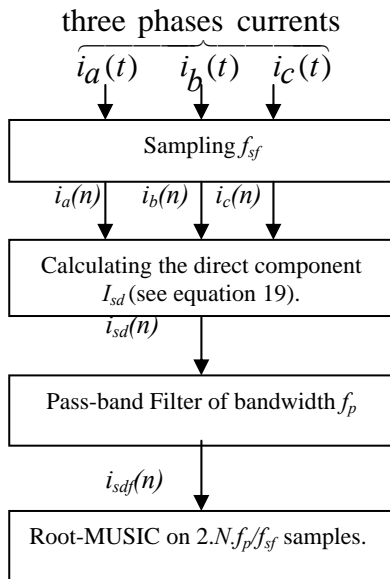


Fig.2. Flowchart of the *RMIF* algorithm

## 5. Experimental Results

Before testing the suggested technique *RMIF* with experimental signals, it is necessary to show the advantage which it gets compared to the *Root-MUSIC* method. For that, we have simulated a signal without noise to determine the computing time in both cases. The signal simulated was sampled at intervals of 1 ms and 4096 samples were used in these simulation. This signal is defined as follows:

$$i_s(n) = 10 \sin(2\pi \cdot \frac{50}{f_{sf}} \cdot n) + 0.3 \sin(2\pi \cdot \frac{45}{f_{sf}} \cdot n) + 0.2 \sin(2\pi \cdot \frac{55}{f_{sf}} \cdot n) \quad (20)$$

Table I gives the results in the case of three harmonics estimation. We notice the important time put for the frequencies estimation and especially the size memory used by *Root-MUSIC* method. Besides, if the harmonics number to be estimated or the data length increases, the computation time and size memory used increases too. This table shows an important reduction of the computing time and memory size with *RMIF* compared to the classical *Root-MUSIC* method. We can thus estimate the same frequencies in a given frequency bandwidth with a very reduced computing time. It is the required advantage. Otherwise, we also notice that there is a small difference in the power estimation. This result is the consequence of the attenuations brought by the band pass filter used.

Method	Data Length	Identification harmonics (Frequencies / Powers)	Memory size used (Bytes)	Computation Time (s)
<i>Root-MUSIC</i>	4096	50.00 Hz / 16.41 dB 44.99 Hz / -14.02 dB 55.00 Hz / -17.57 dB	136.679	276.51
<i>RMIF</i>	164	50.00 Hz / 16.43 dB 45.00 Hz / -13.88 dB 54.99 Hz / -17.19 dB	0.576	0.42

TABLE I: Speed computation comparison

### 5.1. Experimental Set-Up Description

In order to compare the fault detection performance of the two investigated spectrum analysis techniques (*PSD* and *RMIF*), we performed experimental work on an induction motor. The motor used in the experimental investigation is a three phases, 1.1 kW, 50Hz, 2 pole pairs, squirrel cage induction machine. The induction motor is driven by field oriented vector algorithm included in a speed control closed-loop and run under different loads by using a *DC* generator mechanically coupled to the motor [18].

The motor was run and tested with the healthy rotor and with the faulty rotor (one rotor bar fault, then two rotor bars fault). Several rotors of identical type could be interchanged. Each of them is a single squirrel cage type with 28 rotor bars. The broken-bar faults were created by drilling holes in the bars. Before identification, measured variables are passed through a 4th order Butterworth anti-aliasing filter whose cut-off frequency is 500 Hz. Therefore, 17 sets of different data were collected and processed to cover all different torque-speed machine conditions. The stator current data acquisition was done at a sampling period equal to 0,7 ms and each data length is equal to 13347samples [18]. Thus the frequency resolution is equal to:  $\Delta f = \frac{f_{sf}}{N} \approx 0.1\text{Hz}$ .

In this work, we are interested in rotor bar fault detection. Therefore, the study will make itself around the fundamental frequency. The stator current spectrum will be filtered with a pass-band filter. The filter used for *RMIF* is performed by a recursive *IIR* digital filter using a least square fit to specified frequency bandwidth [40 Hz, 60Hz]. Besides, we will use the direct component  $i_{sd}$  (see equation (19)) in the proposed algorithm.

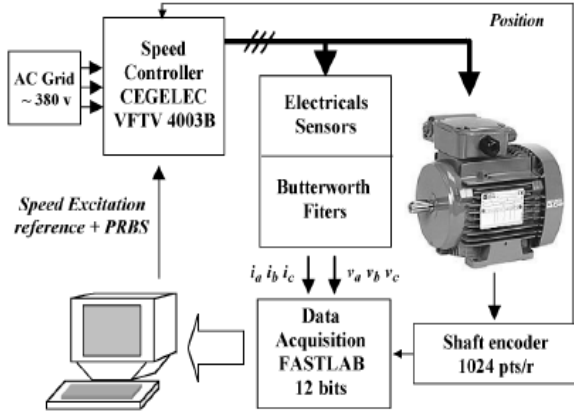


Fig. 3. Motor experimental setup

## 5.2. Experimental Results

### A. Healthy rotor

The motor was initially set with its cage intact. In the absence of broken rotor bar, the behaviour of the motor is mostly characterised by the presence of the fundamental component, 50 Hz in the stator current spectrum. According to figure 4 no harmonics are around the fundamental frequency.

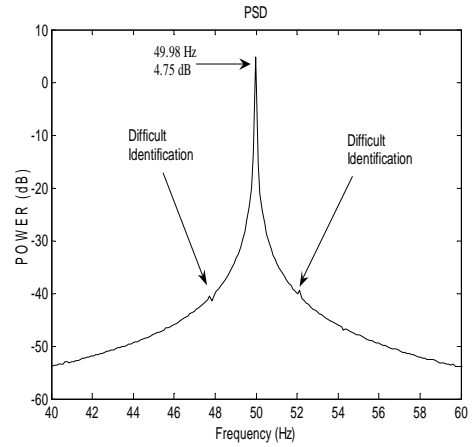


Fig.4. Frequency estimate by *PSD* for the healthy motor.

Table II shows the frequencies and powers estimation by *RMIF*, we can see two sidebands close to the fundamental frequency (47.87 Hz and 52.11 Hz).

$f_i$ (Hz)	47.87	49.97	52.11
Power (dB)	-56.28	4.16	-56.77

TABLE II: Frequencies and powers estimated by *RMIF* for the healthy rotor.

These sidebands are the result of a light natural eccentricity. This is most probably due to inherent stator and rotor asymmetry. The frequencies due to broken rotor bar and eccentricity are identically near to the fundamental frequency [8]. This is why we must make a statement when the rotor is healthy. Thereafter, we will compare the result with this statement for the diagnostic of induction motor. Figure 5 graphically represents the results obtained.

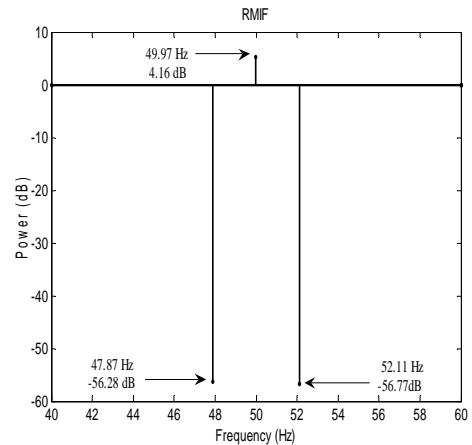


Fig.5. Frequency estimate by *RMIF* for the healthy motor.

### B. One rotor bar fault

In the second test, the measured mechanical speed of the motor is equal to:  $w_r = 1468 \text{ rpm}$ , that is a slip:  $s=0.0213$ . Theoretically, while applying the expression (1) with  $k = 1, \dots, 4$  for  $s=0.0213$ , the 8 frequency components observed can be related to rotor broken bar fault (41.48, 43.61, 45.74, 47.87, 52.13, 54.26, 56.39 and 58.52 Hz). These frequencies are around the fundamental frequency. Table III shows the eight frequencies (plus the fundamental) and powers estimation by *RMIF*. We notice the very good results obtained.

$f_i$ (Hz)	41.65	43.45	45.63	47.81	49.99
Power (dB)	-69.19	-63.79	-54.12	-38.92	4.34
$f_i$ (Hz)	52.16	54.34	56.52	58.71	
Power (dB)	-39.37	-51.86	-64.08	-69.59	

TABLE III: Frequencies and powers estimated by *RMIF* for one rotor bar fault.

Figure 6 represents the layout of the stator current spectrum by the *PSD* technique. We notice that the small harmonics are not detectable (41.48, 43.61, 56.39 and 58.52 Hz).

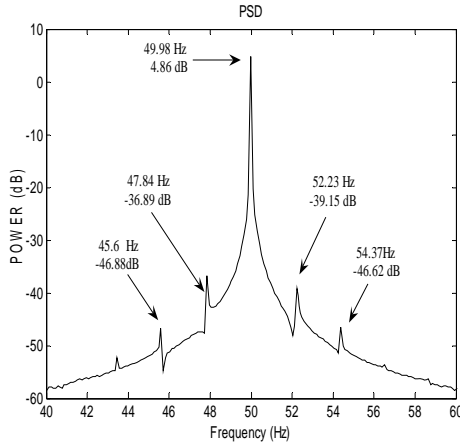


Fig.6. Frequency estimate by *PSD* for one rotor bar fault.

*RMIF* technique estimates all harmonics possible in the specified bandwidth (see Figure 7). Moreover, we notice especially the clearness of the representation by the suggested technique.

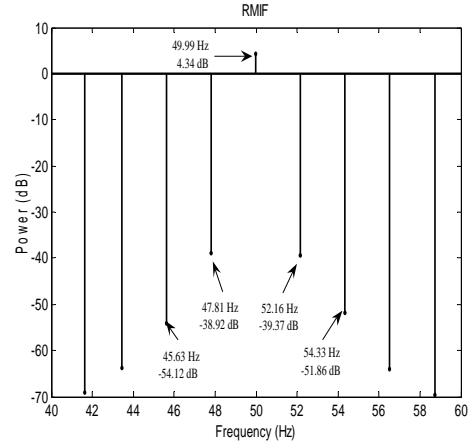


Fig.7. Frequency estimate by *RMIF* for one rotor bar fault.

### C. Two rotor bars fault:

In this case, the measured mechanical speed of the motor is equal to:  $w_r = 1458 \text{ rpm}$ . We notice a little variation of speed. In this condition, the slip becomes:  $s=0.028$ . Theoretically for this slip, we have 6 frequency components related to rotor broken bar fault (41.2, 44.4, 47.2, 52.8, 55.6, 58.4 Hz). Table IV shows the frequencies and powers estimation by *RMIF*.

$f_i$ (Hz)	41.72	44.47	47.22	49.99
Power (dB)	-56.36	-51.31	-31.12	5.06
$f_i$ (Hz)	52.74	55.49	58.22	
Power (dB)	-30.63	-45.71	-53.68	

TABLE IV: Frequencies and powers estimated by *RMIF* for two rotor bars fault.

We have good harmonics estimation by *PSD*, nevertheless this method could not detect the very low powers harmonics (see Figure 8). Whereas when the *RMIF* technique is used, all detectable harmonics can be estimated within the specified bandwidth. It is the merit that this technique has compared to the *PSD* method (see Figure 9). According to the results obtained, we also notice that the powers of the various harmonics increased with the number of broken bars. Thus a good estimate of the powers enables us to estimate the number of broken bars.

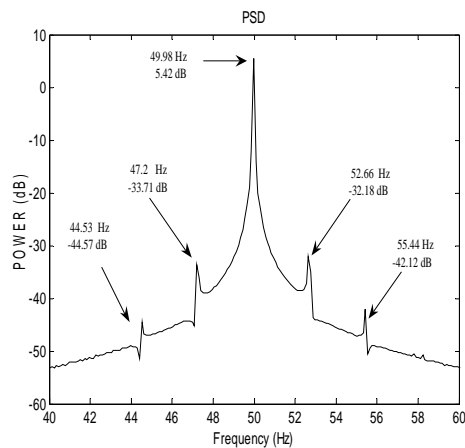


Fig.8. Frequency estimate by PSD for two rotor bars fault.

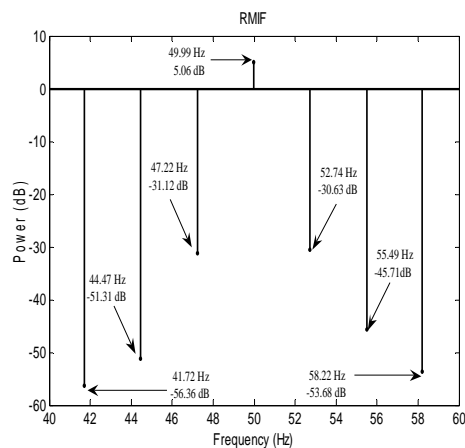


Fig.9. Frequency estimate by RMIF for two rotor bars fault.

## 6. Conclusion

The *Root-MUSIC* method is a powerful tool for detecting frequencies, but this method has the inconvenience of long computation time when a large frequency signal dimension or a large number of samples are requested. The proposed *RMIF* algorithm is a technique to overcome this problem and to make the *Root-MUSIC* faster and more accurate in extracting frequencies in a specified bandwidth. This advantage, will allow the possible use of this technique in on-line diagnosis. Moreover, the statistical results based on experimental data clearly indicate that *RMIF* technique has better discrimination capability and is more robust compared to *PSD* method. These results also prove that *RMIF* technique is very effective in the case of incipient rotor fault. We can also notice that the harmonics powers increase with the number broken bars, which lead to a very interesting and useful

results for the faults characterization. To validate this result, extensive experimental studies are necessary to assess fully the usefulness and effectiveness of the proposed technique.

## Acknowledgements

The authors wish to thank all the team of the Laboratory of Automatic and Industrial Informatics of the University of Poitiers FRANCE and special thanks to Mr. Gerard Champenois and Mr. Smail Bachir for the aid they afforded for our experimental work validation.

## References

- [1] Bendiabdellah A., Benouzza N., Toumi D.: *Cage rotor Faults detection by speed estimation and spectral current analysis*. The 3<sup>rd</sup> IET International Conference on Power electronics, Machines and Drives (PEMD 2006), April 4-6, 2006, Dublin Ireland.
- [2] Bonnet A.H., Soukup G.C.: *Cause and Analysis of Stator and Rotor Failures in Three-Phase Squirrel-Cage Induction Motors*. IEEE Trans. Ind. Applications, 1992, vol. 28, n.4, pp.921-937.
- [3] Ayhan B., Chow M.Y., Trussell H.J., Song M.H: *A case on the Comparison of non-parametric spectrum methods for broken rotor bar fault detection*. The 29th Annual Conference of the IEEE, IECON '03, Nov 2-6, 2003, vol.3, pp.2835-2840.
- [4] Kia S.H., Henao H., Capolino G.A.: *Zoom-MUSIC frequency estimation method for three phase induction machine fault detection*. The 32nd Annual Conference of IEEE, IECON 2005, Nov 6-10, 2005, pp.2603-2608.
- [5] Benbouzid M.E.H, Nejari H., beguenane R., Vieira M.: *Induction motor asymmetrical faults detection using advanced signal processing techniques*. IEEE Trans. Energy conversion vol. 14, n. 2, June 1999.
- [6] Kliman G.B. and al.: *Non-invasive detection of broken rotor bars in operating induction motors*. IEEE Trans. On Energy Conversion, 1988, vol. EC-3, n. 4, pp. 873-879.
- [7] Elkasabgy N.M., Eastham A.R., Dawson G.E.: *Detection of broken bars in the cage rotor on an induction machine*. IEEE Trans. on Industrial Applications, Jan-Feb 1992, vol. IA-22, n°6, pp. 165-171.
- [8] Didier G., Razik H., Rezzoug A.: *On the experiment detection of incipient rotor fault of an induction motor*. Electric Machines and Drives Conference, IEMDC'03, June 1-4 2003, vol. 2, pp. 913-913.
- [9] Cupertino F., Martorana G., Salvatore L., Stasi S.: *Diagnostic start-up test to detect induction motor broken bars via Short-Time MUSIC algorithm applied to current Space-Vector*, EPE'03, September 2-4 2003, Toulouse France.

- [10] Marple S. L.: *Digital Spectral Analysis with Applications*. Prentice-Hall Signal processing Series, 1987.
- [11] Hayes M.H.: *Statistical digital signal processing and modelling*. John Wiley & Sons, New-York, 1991.
- [12] Boudinar A.H.: *Déconvolution des signaux ultrasonores appliquée à l'imagerie*. Master Thesis. Dept. Electronic, University of Sciences and Technology of Oran, Algeria. June 1997.
- [13] Marcos S. : *Méthodes haute résolution*. Hermes, Paris, 1998.
- [14] Cover T.M., Thomas J.A.: *Elements of Information Theory*. John Wiley & Sons, New-York, 1991.
- [15] Akaike H.: *A new look at the statistical model identification*. IEEE Trans. Autom. Control, Dec 1974, vol.AC-19,pp 716-723.
- [16] Rissanen J.: *Modeling by shortest data description*. Automatica. 1978, vol.14, pp.465-471.
- [17] Casimir R.: *Diagnostic des défauts des machines asynchrones par reconnaissance des formes*. Ph.D thesis. Ecole doctorale de Lyon, France, Dec 2003.
- [18] Bachir S., Tnani S., Trigeassou J.C., Champenois G.: *Diagnosis by parameter estimation of stator and rotor faults occurring in induction machines*. EPE'01, Graz, Autriche, August 2001.



**Nouredine Benouzza** was born on August 17, 1963 in Oran Algeria. He received his B.S Engineering degree, M.S degree and Ph.D degree from the University of Sciences and Technology of Oran, Algeria, in 1989, 1993 and 2006 respectively.

He is currently Professor of Electrical Engineering at the University of Sciences and Technology of Oran, (USTO) Algeria. His research interests include: Electrical machines and Drives Control, as well as Electrical machines Faults Diagnosis.



**Nabil BOUGHANMI** was born on December 20, 1963 in Oran Algeria. He received his B.S Engineering degree from the University of Sciences and Technology of Oran, Algeria, in 1986, and Ph.D degree from the "Institut Natinal Polytechnique" of Toulouse, France

in 1991. He is currently Professor of Electronic Engineering at the University of Sciences and Technology of Oran, (USTO) Algeria. His research interests include: Signal and Image processing.

#### Authors' information



**Ahmed Hamida BOUDINAR** was born on September 10, 1969 in Oran Algeria. He received his B.S Engineering degree, M.S degree from the University of Sciences and Technology of Oran, Algeria, in 1992, 1997 respectively. He is currently Professor of Electrical

Engineering at the University of Sciences and Technology of Oran, (USTO) Algeria. His research interests include: Numerical Methods for signal processing, as well as Electrical machines Faults Diagnosis.



**Azeddine Bendiabdellah** was born on January 10, 1958 in Saida Algeria. He received his Bachelor Engineering degree with honours and his Ph.D degree from the University of Sheffield, England, in 1980, and 1985 respectively. From 1990 to 1991 he was a visiting

professor at Tokyo Institute of Technology (T.I.T), Japan. He is currently Professor of Electrical Engineering at the University of Sciences and Technology of Oran, (USTO) Algeria. His research interests include: Electrical machines Design and Drives Control and Converters; for Field Calculations, as well as Electrical machines Faults Diagnosis.